石 油 学 报

（石油加工）

第 34 卷 第 5 期 2018 年 9 月

目 次

研究报告

第十九届全国分子筛学术大会论文专栏

信息

* 封面文章

期刊基本参数：CN11－2129/TE * 1985 * b * A4 * 208 * zh＋en * P * ￥20.00 * 1200 * 26 * 2018－09 **本期责任编辑**：黄晓晖

ACTA PETROLEI SINICA

(PETROLEUM PROCESSING SECTION)

Vol .34 No .5 Sep. 2018

CONTENTS

Research Articles

Acta Petrolei Sinica (*Petroleum Processing Section*), 2018, 34(5): 0849-0855 **doi**: 10.3969/j.issn.1001-8719.2018.05.001

Hydrodesulfurization Performance of Zeolite-Containing CoMoP/Al_2O_3 Catalysts

LIU Shizhe LI Mingfeng WANG Yongrui ZHANG Le
YANG Ping LI Dadong

The catalytic activity and product selectivity via different reaction pathways over CoMoP/Al_2O_3-zeolite catalysts were influenced by both pore structure and the accessibility of acid sites of zeolites. Compared with CoMoP/Al_2O_3 and other CoMoP/Al_2O_3-zeolite catalysts, CoMoP/Al_2O_3-Y exhibits the highest conversion and sulfur removal rate of 4,6-DMDBT.

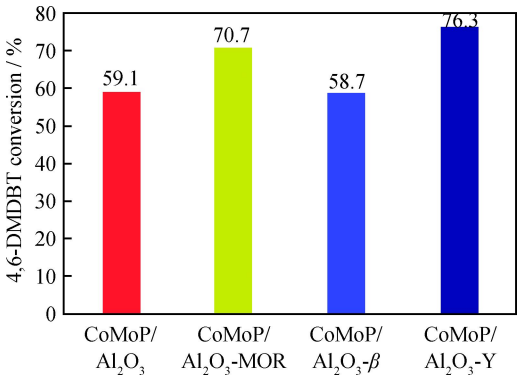

Acta Petrolei Sinica (*Petroleum Processing Section*), 2018, 34(5): 0856-0862 **doi**: 10.3969/j.issn.1001-8719.2018.05.002

Coke Formation Caused by Non-basic Nitrogen Compound in Catalytic Cracking Process

LI Fuchao WANG Di ZHANG Jiushun WEI Xiaoli

Comprehensive analytical techniques were applied to characterize the detailed composition and structure of coke, which results from indole. Results show that more than 60 percent of Lewis acid sites are deactivated comparing with Brönsted acid sites. The study also reveals that most of nitrogen-containing coke is formed in the earlier stage of cracking while hydrocarbons are the primary contributors to coke yield in high conversion.

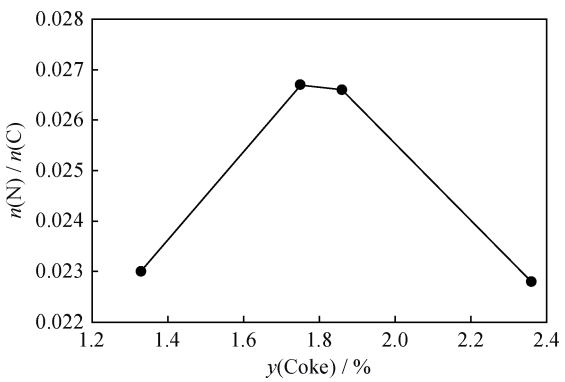

Acta Petrolei Sinica (*Petroleum Processing Section*), 2018, 34(5): 0863-0871 **doi**: 10.3969/j.issn.1001-8719.2018.05.003

Preparation and Characterization of Ultrastable Mesoporous Silicated Alumina and Its Application in Catalytic Cracking

SHI Zongbo WANG Yimeng

The silicated alumina shows high activity in the cracking of hydrocarbon, and its crystal structure and cracking activities are well preserved after calcination at 800℃ for 4 h in steam or at 1100℃ for 6 h in air.

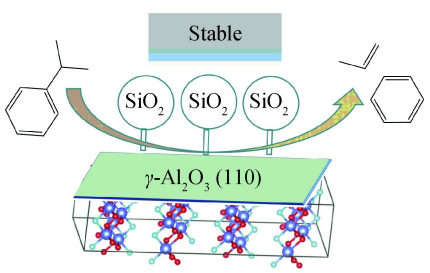

Acta Petrolei Sinica (*Petroleum Processing Section*), 2018, 34(5): 0872-0881 **doi**: 10.3969/j.issn.1001-8719.2018.05.004

Effect of Si/Al Ratio on the Catalytic Performance of ZSM-5 Zeolite in Alkane and Cycloalkane Cracking

HAN Lei OUYANG Ying XING Enhui LUO Yibin DA Zhijian

The acid-treated ZSM-5 zeolites with different $n(SiO_2)/n(Al_2O_3)$ were prepared by post treatment method. ZSM-5 zeolites with different $n(SiO_2)/n(Al_2O_3)$ show different catalytic performance in hydrocarbon catalytic cracking. With respect to the same carbon number of octane and ethylcyclohexane, the appropriate $n(SiO_2)/n(Al_2O_3)$ needed is different, due to the difference among various molecules.

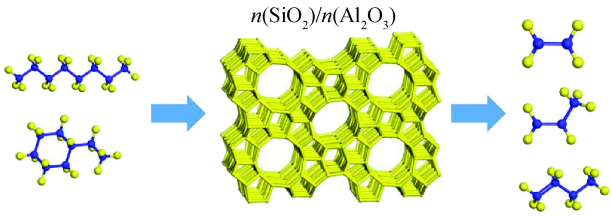

Acta Petrolei Sinica (*Petroleum Processing Section*), 2018, 34(5): 0882-0890 **doi**: 10.3969/j.issn.1001-8719.2018.05.005

Synthesis of Carbon and Metal-Doped Porous Boron Nitride: Adsorbents for Sulfur Removal From Diesel

WANG Yanzhen LI Ruijie SONG Chunmin DUAN Hongling GAO Wenluan XIE Songwei

Novel carbon and metal-doped step-like BN mesoporous materials with high specific surface area have been prepared. The carbon and metal-doped BN display significantly higher amount of acid sites and a much better adsorptive performance than the pure carbon-doped BN. Moreover, it is the first time that metal-doped BN applies in adsorptive desulfurization.

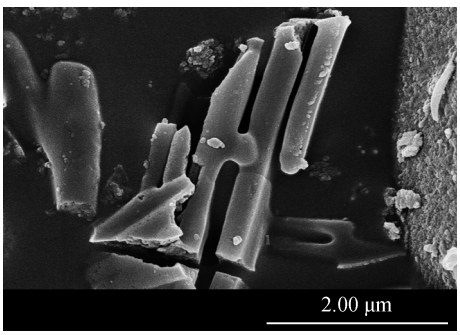

CBN

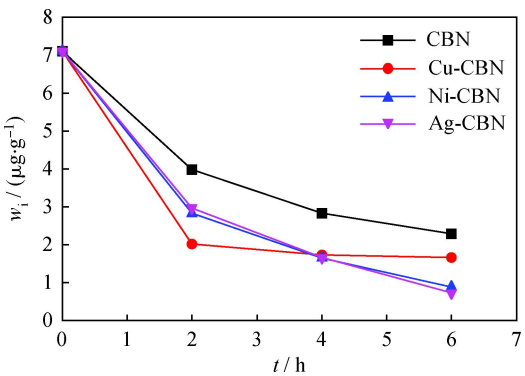

Acta Petrolei Sinica (*Petroleum Processing Section*), 2018, 34(5): 0891-0896 **doi**: 10.3969/j.issn.1001-8719.2018.05.006

Synthesis of ZSM-5 Zeolite by Glycerin-Assisted Seed Crystallization Method

LIU Yu HAN Shunyu CAO Cuiping ZHANG Huanhuan LIU Weiying JIANG Nanzhe

ZSM-5 zeolite was hydrothermally synthesized by glycerin-assisted seed crystallization method. The appropriate amount of glycerol can increase the relative crystallinity of ZSM-5 zeolite, and inhibit the generation of α-SiO_2, thus increasing the specific surface area.

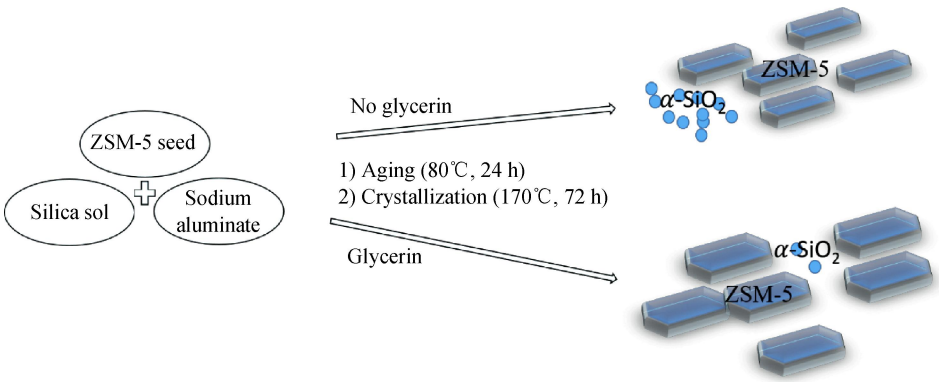

Acta Petrolei Sinica (*Petroleum Processing Section*), 2018, 34(5): 0897-0903 **doi**: 10.3969/j.issn.1001-8719.2018.05.007

Carbon Dioxide Hydrogenation With Glycerol Over Ru-MACHO Catalysts

SHEN Zheng WANG Chenlu LIU Shiyang ZHANG Wei HUANG Xin ZHANG Yalei

Herein, Ru-MACHO (regR) has been chosen as catalyst to promote the performance of CO_2 hydrogenation with glycerol, contributing to the efficient hydrogenation of CO_2 to formic acid and meantime the dehydrogenation of glycerol to lactic acid.

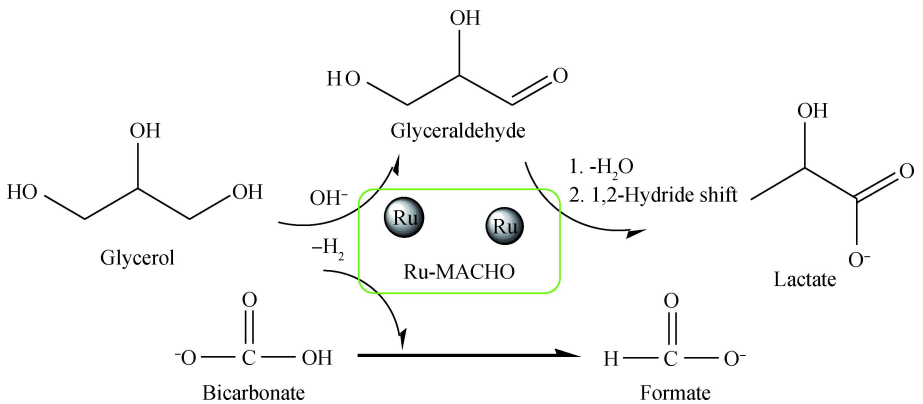

Acta Petrolei Sinica (*Petroleum Processing Section*), 2018, 34(5): 0904-0911 **doi**: 10.3969/j.issn.1001-8719.2018.05.008

Hydrodeoxygenation of Fatty Acid Methyl Esters Catalyzed by Pt/ZSM-5-Al_2O_3

WU Yu LIU Xuejun ZHANG Yi JING Yicao WANG Hongwei JI Jianbing

The methyl group attached to the ester molecules is firstly broken due to the presence of the p-π conjugate system in the FAME. Furthermore, the n-alkane is obtained by hydrodeoxygenation and decarbonylation/decarboxylation reactions. The diesel components yield is maximized at 340℃

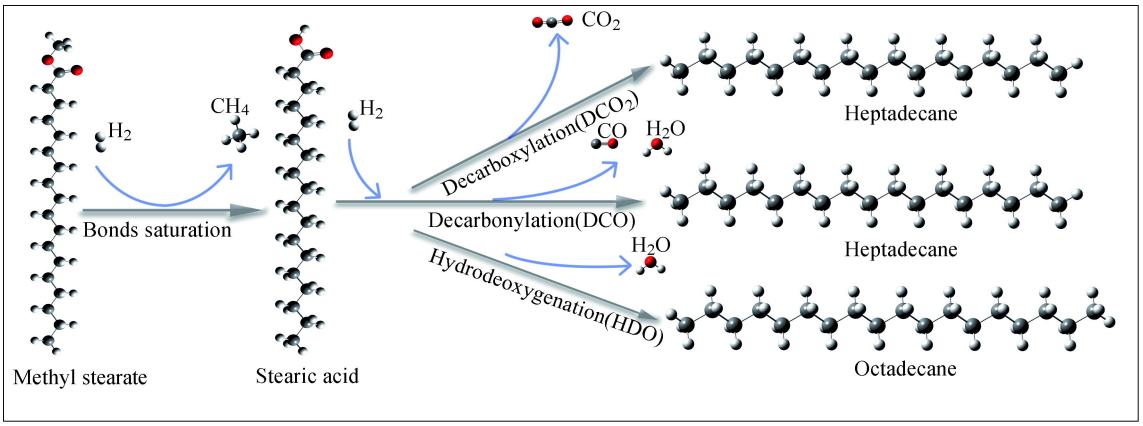

Acta Petrolei Sinica (*Petroleum Processing Section*), 2018, 34(5): 0912-0919 **doi**: 10.3969/j.issn.1001-8719.2018.05.009

Preparation of Fe_2O_3-CeO_2 Photocatalyst and Its Catalytic Performance

LI Youfeng LIU Guoqing ZENG Lingwei PENG Zhenshan
XIANG Xiangyu WANG Ying HUANG Xiao

When the catalyst mass concentration is 100 mg/L, pH=10.0 and the photocatalytic time is 100 min, the maximum degradation rate of methylene blue using Fe_2O_3-CeO_2 catalyst prepared by coprecipitation method reaches 97.6%. While that is 93.4% when Fe_2O_3-CeO_2 prepared by impregnation method with catalyst mass concentration of 50 mg/L, and that is 75.8% catalyzed by pure CeO_2.

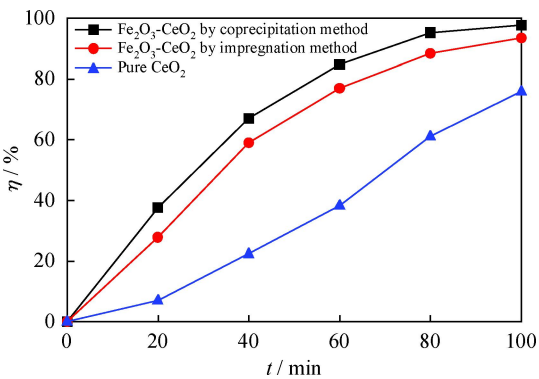

Acta Petrolei Sinica (*Petroleum Processing Section*), 2018, 34(5): 0920-0928 **doi**: 10.3969/j.issn.1001-8719.2018.05.010

Adsorption Simulation of Coke Precursors in Isobutene/Butane Alkylation Over Y Zeolite

DU Yannian ZHOU Xiang ZHOU Han GUO Jinbiao

Coke precursors generated in isobutane/butene alkylation process have different adsorption capabilities, which can be observed on the differences of their adsorption energy and stable adsorption conformation in Y zeolite. The straight chain coke precursor compounds occupy two-dimensional space in Y zeolite channel after adsorption, and the cyclic coke precursor compounds occupy three-dimensional space in Y zeolite channel. Especially, bicyclic coke precursor compounds have more serious pore blocking effect.

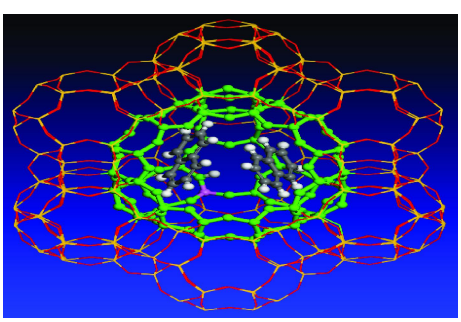

Acta Petrolei Sinica (*Petroleum Processing Section*), 2018, 34(5): 0929-0941 **doi**: 10.3969/j.issn.1001-8719.2018.05.011

Temperature Control Start-up of Divided Wall Column Pilot Plant Used for Aromatic Reformate Separation

WU Hao SHEN Benxian HUA Tao QIU Jie LING Hao

This work proposed a start-up procedure of DWC pilot plant using four temperature control loops. The automatic start-up procedure was firstly simulated by Aspen Dymamics, and then been tested on the DWC pilot plant. Test results show that, at the end of automatic start-up process, the composition profiles of the DWC matched very well with the results from the Aspen Plus steady state simulation.

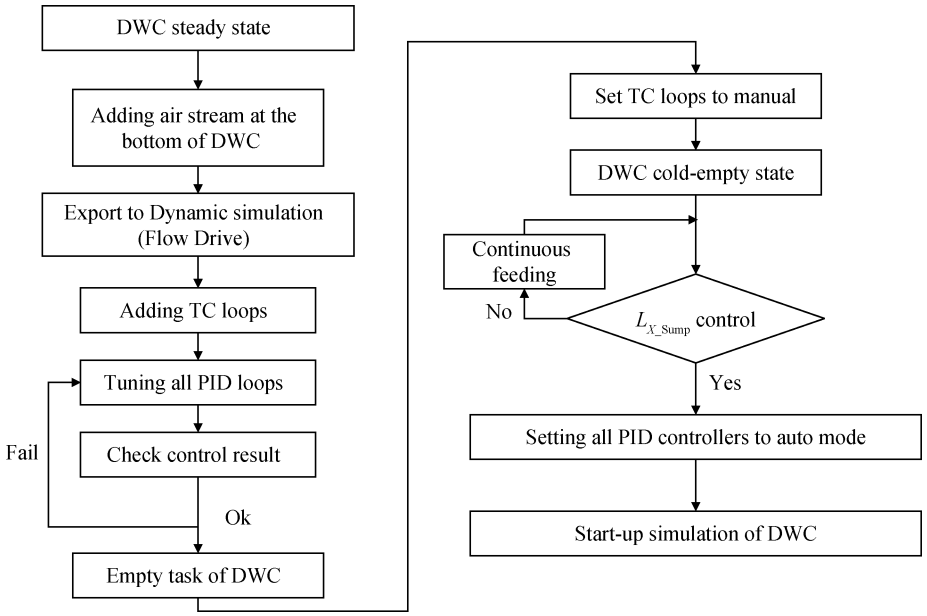

Acta Petrolei Sinica (*Petroleum Processing Section*), 2018, 34(5): 0942-0950 **doi**: 10.3969/j.issn.1001-8719.2018.05.012

Pressure Characteristics in the Ring Space Downward Pipe of a Novel MTO Reactor

WANG Fenfen YAN Xiao E Chenlin LU Chunxi

This is the schematic graph of a loop reactor for MTO process. The feedstock is simultaneously passed to the draft tube and annulus region containing catalysts to effect a majority of conversion to light olefins and then passed to the separation zone. This structure enables the particles in the downward pipe of the ring space above to flow stably.

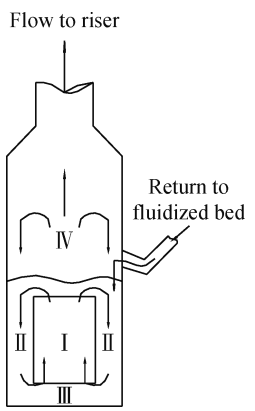

Ⅰ—Draft tube region; Ⅱ—Annulus region; Ⅲ—Bottom region; Ⅳ—Gas-solid separation region

Acta Petrolei Sinica (*Petroleum Processing Section*), 2018, 34(5): 0951-0958 **doi**: 10.3969/j.issn.1001-8719.2018.05.013

Simulation and Optimization of Coal Tar Chemical Looping Pyrolysis Process

GONG Mingxin WANG Cuiping GUO Qingjie LI Yongpeng GONG Jian

The detailed process of coal tar chemical looping pyrolysis with iron-oxide oxygen carrier was built in ASPEN PLUS software according to experimental work. Carbon black yields, coal tar conversion ratio, syngas ratio and energy conversion efficiency were the objective parameters to optimize the process and operation conditions.

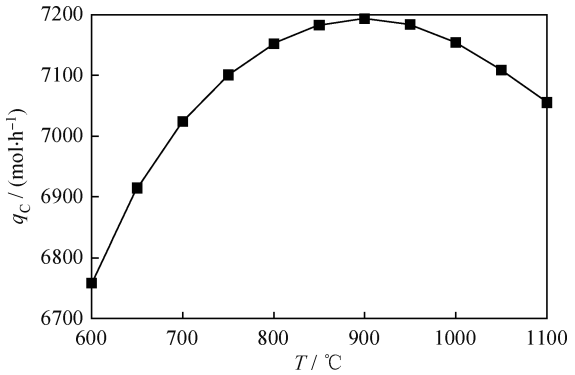

Acta Petrolei Sinica (*Petroleum Processing Section*), 2018, 34(5): 0959-0966 **doi**: 10.3969/j.issn.1001-8719.2018.05.014

Effect of Diesel Soot on Friction Reducing Performance of Organo-Molybdenum Friction Modifier

XIONG Yun SU Peng LIU Xiao YANG He

The anti-friction of two kinds of organo-molybdenum friction modifier M1 and M2 were investigated by using cylinder-disc reciprocating mode on the SRV IV oscillating reciprocating friction and wear tester in diesel engine oil with and without diesel soot. Diesel soot could significantly reduce the anti-friction property of organo-molybdenum friction modifier. M1 has better anti-friction property than M2 in diesel soot contaminated engine oil.

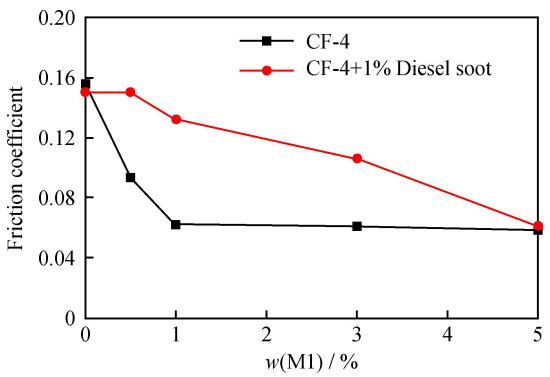

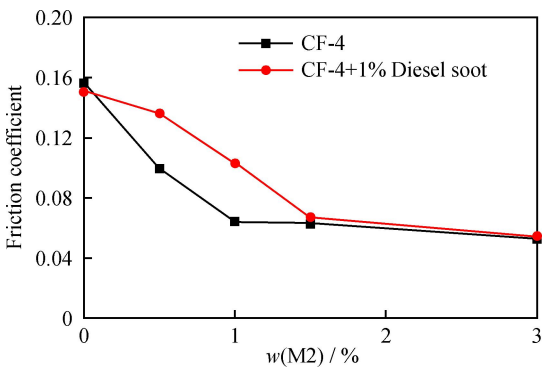

Acta Petrolei Sinica (*Petroleum Processing Section*), 2018, 34(5): 0967-0974 **doi**: 10.3969/j.issn.1001-8719.2018.05.015

Numerical Study of the Effect of Stokes Number on Particles Deposition Characteristics in FCC Flue Gas Turbines

PAN Jingna WANG Jianjun CHEN Shuaifu XU Shugen

A critical stress model is proposed with considering the effect of particle-wall surface adhesion. Particles with small Stokes number are easy to be deposited, and thus these particles should be avoided to enter flue gas turbine to ensure its safe and long-term operation.

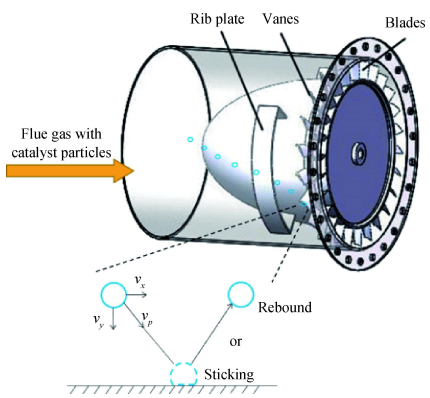

Acta Petrolei Sinica (*Petroleum Processing Section*), 2018, 34(5): 0975-0980 **doi**: 10.3969/j.issn.1001-8719.2018.05.016

Effect of Row Number in Longitudinal Vortex Generator on Gas-Solid Two Phase Flow in Three Dimensional Spouted Bed

ZHANG Jiejie SHANG Lingyi WU Feng MA Xiaoxun YANG Jian

Longitudinal vortices can effectively increase particle volume fraction near annulus region in the spouted bed. It can also significantly enhance the radial velocity of particle phase in the spouted bed, strengthen the radial mixing of gas phase and particle, and thus effectively reduces the granular temperature.

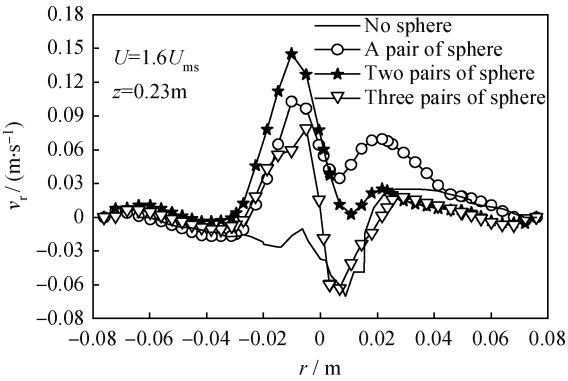

Acta Petrolei Sinica (*Petroleum Processing Section*), 2018, 34(5): 0981-0986 **doi**: 10.3969/j.issn.1001-8719.2018.05.017

Identification of Meso-Scale Flow Structure in a Dense Phase Gas-Solid Fluidized Bed

LI Zhipeng NIU Li LIU Mengxi

A third moment analysis method is employed to decouple the transient signals registered in a fluidized bed. It is identified the bubble phase threshold value is in a range of 0.26—0.35. The agglomerates have a mean solid holdup from 0.55 to 0.555 and appear at a frequency of 0.5 Hz to 3.2 Hz.

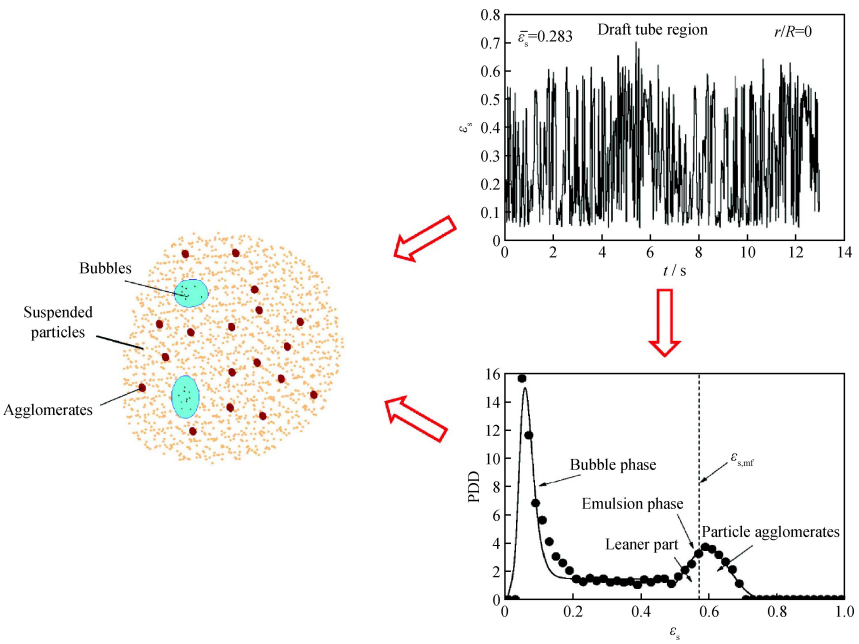

Acta Petrolei Sinica (*Petroleum Processing Section*), 2018, 34(5): 0987-0994 **doi**: 10.3969/j.issn.1001-8719.2018.05.018

Study on Density Uniformity in a Deep Air Dense Medium Fluidized Bed

LI Guofeng DUAN Chenlong LU Junyu ZHAO Yuemin ZHOU Enhui

This paper mainly studied the radial non-uniform distribution of density in a deep air dense medium fluidized bed, and the effects of air chamber structure and operation parameters. Research results indicate that the deep bed density under the traditional air chamber has a convex distribution, whereas a concave and more uniform distribution has been observed for the new-type chamber.

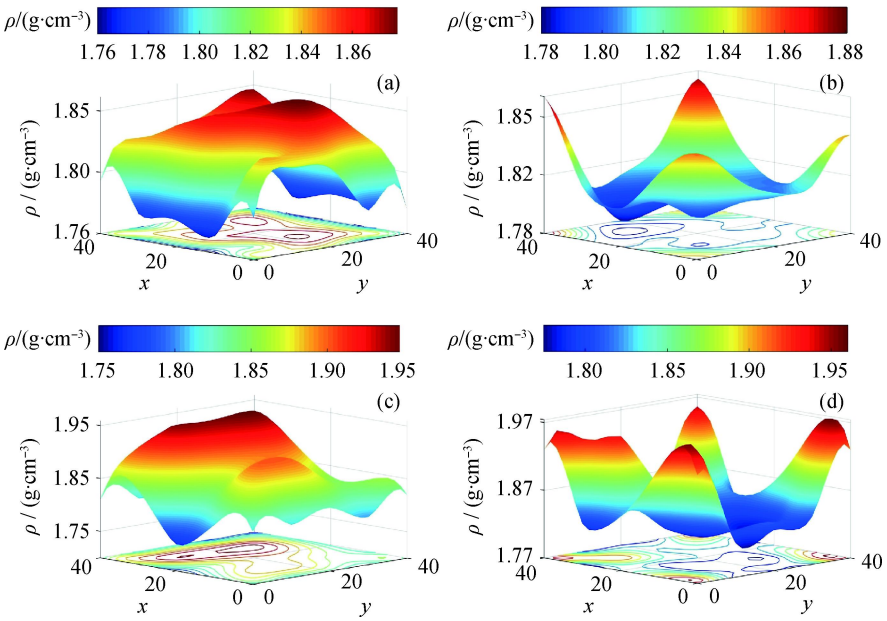

(a) H_s=600 mm, Traditional air chamber; (b) H_s=600 mm, New-style air chamber;
(c) H_s=680 mm, Traditional air chamber; (d) H_s=680 mm, New-style air chamber;
x-axis and *y*-axis are the reference axes of the tested points in the fluidized bed

Acta Petrolei Sinica (*Petroleum Processing Section*), 2018, 34(5): 0995-1003 **doi**: 10.3969/j.issn.1001-8719.2018.05.019

Effects of PEG and TMB-5 on the Crystallization and Properties of PLLA

WU Xuejian LUO Faliang QI Yaping XING Qian
WANG Kezhi

The glass transition temperature of PLLA/TMB-5/PEG blends gradually reduced with increasing of PEG content. PLLA/TMB-5/PEG blends of glass transition temperature optimal when mass fraction of PEG reached 4%, which of PLLA/TMB-5 blends were reduced by 7.7℃.

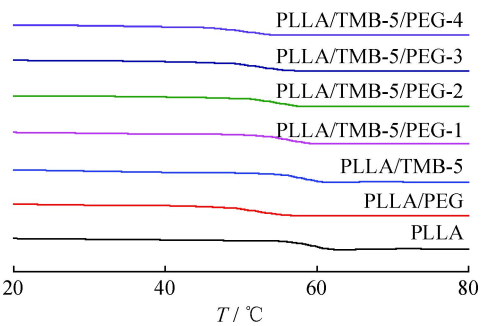

Acta Petrolei Sinica (*Petroleum Processing Section*), 2018, 34(5): 1004-1012 **doi**: 10.3969/j.issn.1001-8719.2018.05.020

Dynamic Multi-Point Fault Monitoring Method for Multi-Model Chemical Process

HU Jinqiu LUO Jing GUO Fang

The chemical process was divided into stationary mode and transition mode, the single-point monitoring statistic and the multi-point anomaly statistic of the stationary mode were constructed based on the independent component analysis algorithm of the autoregressive model and particle swarm optimization, and the non-Gaussian monitoring model of the transition mode was structured based on the particle swarm optimization-Independent component analysis algorithm. On-line fault monitoring can be realized by both the above two monitoring models.

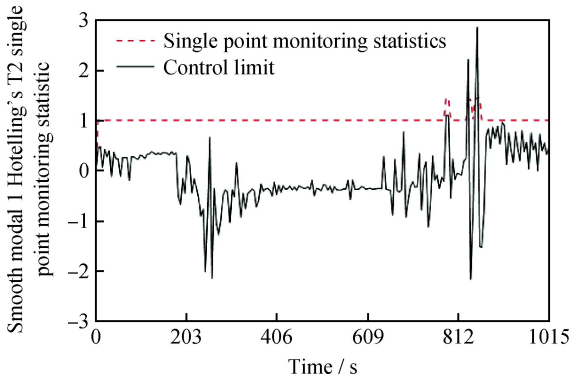

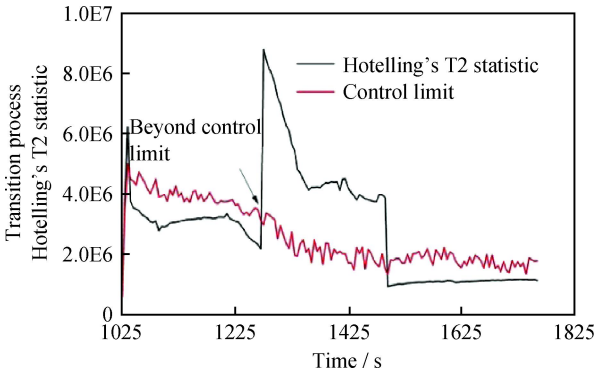

The 19th Chinese Zeolite Conference Articles

Acta Petrolei Sinica (*Petroleum Processing Section*), 2018, 34(5): 1013-1019 **doi**: 10.3969/j.issn.1001-8719.2018.05.021

Study on Catalytic Performance of Nanosheet MFI Structured Zeolite in *n*-Hexane Cracking

JI Yajun YANG Honghui YAN Wei

Compared with the conventional ZSM-5 zeolite, nanosheet MFI typed zeolite has larger mesoporous volume and unique ultrathin lamellar structure, which favors the conversion of *n*-hexane and selectivity of propylene in *n*-hexane cracking.

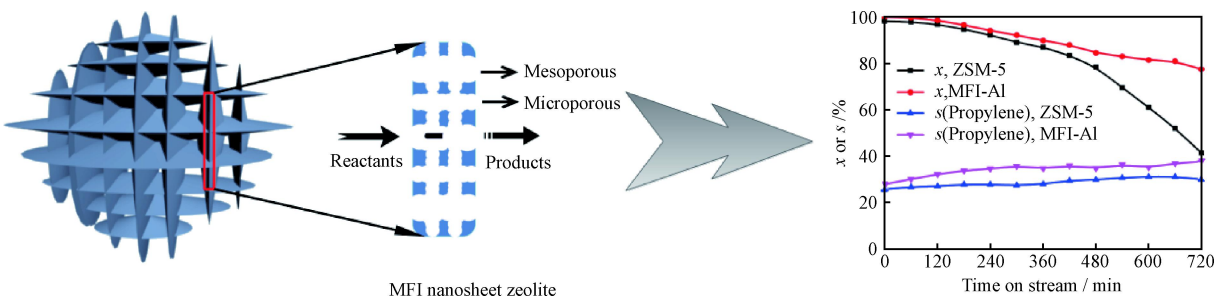

Reaction conditions: *m*(Catalyst)=150 mg; Reaction temperature 650℃; N_2 flow rate 30 mL/min; *n*-Hexane flow rate 3.00 g/h

Acta Petrolei Sinica (*Petroleum Processing Section*), 2018, 34(5): 1020-1026 **doi**: 10.3969/j.issn.1001-8719.2018.05.022

Effect of Accessibility of Brönsted Acid Sites of Zeolites on Adsorption and Reaction Performance of Thiophene

MO Zhousheng QIN Yucai PEI Tingting WANG Lin SONG Lijuan

Due to high accessibility of Brönsted acid sites, Hβ has strong ability to catalyze the conversation of thiophene, which is much higher than that of HMOR and HY. The high accessibility arises from its two vertical 12-MR channels.

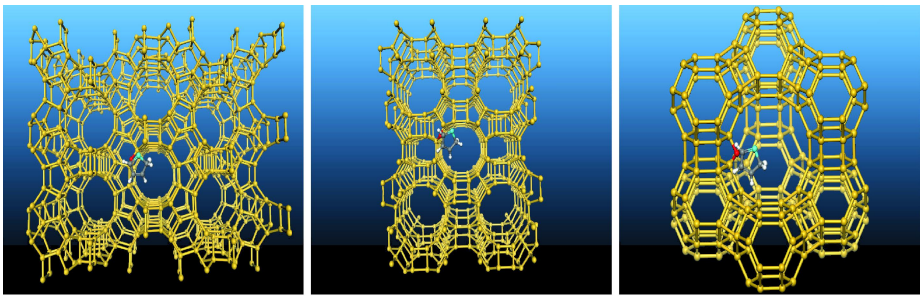

Hβ HMOR HY

Acta Petrolei Sinica (*Petroleum Processing Section*), 2018, 34(5): 1027-1032 **doi**: 10.3969/j.issn.1001-8719.2018.05.023

Hydrocracking Performance and Synthesis of Small Crystal Y Zeolite

YUAN Xiaoliang WANG Yan ZHANG Zhanquan YU Yinglong
ZHANG Zhihua

Small crystal line Y zeolites were synthesized and modified, which show higher crystallinity, higher Si/Al ratio, more moderate acidity and secondary pore. The hydrocracking catalyst using modified zeolite Y as the acid component exhibits better activity and more excellent product distribution.

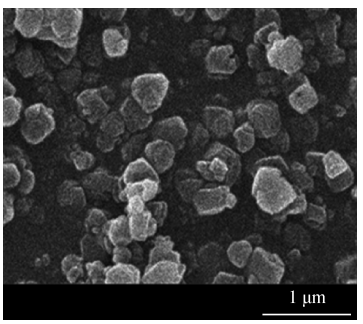

Acta Petrolei Sinica (*Petroleum Processing Section*), 2018, 34(5): 1033-1039 **doi**: 10.3969/j.issn.1001-8719.2018.05.024

Influence of Different Synthesis Conditions in the Presence of Polyethylene Glycol on the Morphology of Hierarchical ZSM-5

ZHANG Jianmin WANG Gaiping LI Hongji CHEN Zhe BAI Mingxin

Several reaction parameters, such as Si/Al ratio, crystallization temperature and time, affect the crystal morphology of ZSM-5 zeliote, which is closely related to the templating role of polyethylene glycol.

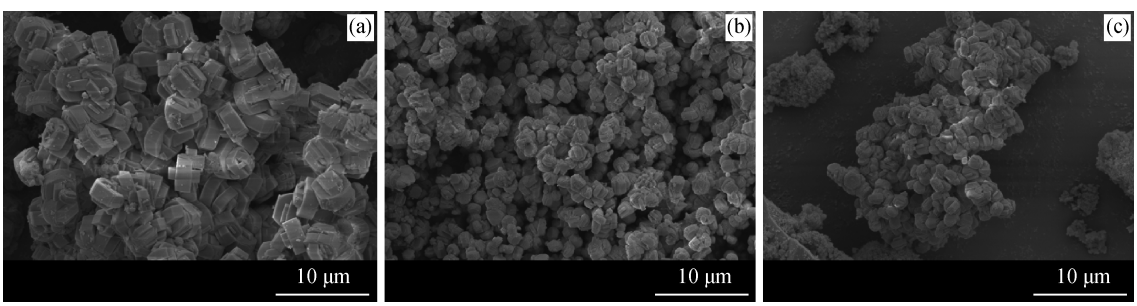

m(Si)/m(Al)/m(PEG): (a) 100/0.027/10; (b) 100/0.027/20; (c) 100/0.027/30

Acta Petrolei Sinica (*Petroleum Processing Section*), 2018, 34(5): 1040-1046 **doi**: 10.3969/j.issn.1001-8719.2018.05.025

Production and Industrial Application of MCM-49 Zeolite

DENG Guangjin LI Jing LÜ Jianhui ZHAO Yin LI Zheng
LIU Xianwu YANG Jixue XU Huili

MCM-49 zeolites were produced in a 8 m^3 high-pressure reactor. Results show that the highly qualified MCM-49 zeolites can be obtained under certain conditions, and the optimal conditions are as following: gelation time of 1 h, crystallization temperature of 140℃ to 160℃, crystallization time of 60 h. The MCM-49 zeolite has been used for 130 thousand tons / a production process of phenol and acetone. And the activity of MCM-49 zeolites meets the requirements of industrial applications. It can reduce the energy consumption, saving 0.691 t/h of steam.

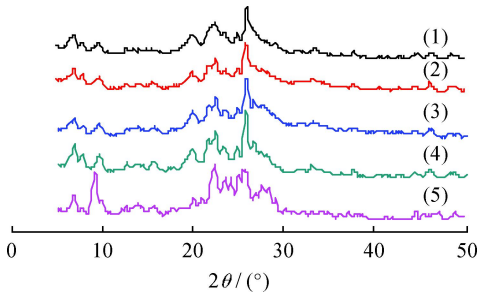

Crystallization temperatures/℃: (1) 140; (2)156; (3)160; (4) 168; (5)172

Acta Petrolei Sinica (*Petroleum Processing Section*), 2018, 34(5): 1047-1056 **doi**: 10.3969/j.issn.1001-8719.2018.05.026

Application of Biochar in Removal of Organics and Heavy Metals From Water

LI Xiangping WANG Chuanbin ZHANG Jianguang LIU Bin
LIU Juping CHEN Guanyi

Biochars obtained by pyrolysis of different biomass are efficient adsorbents for the removal of heavy metals and organic pollution in water. Biochar from different sources has a certain bias to the adsorption of pollutants in water.